POLITECNICO
MILANO 1863

SCUOLA DI INGEGNERIA INDUSTRIALE
E DELL'INFORMAZIONE

Executive Summary of the Thesis

CFD study for the optimization of a mixing pipe for SCR system

Laurea Magistrale in Mechanical Engineering - Ingegneria Meccanica

Author: Antonio Maisto 244883

Advisor: Prof. Augusto Della Torre

Co-advisor: Mattia Pelosin

Academic year: 2024-2025

1. Introduction

Over the last decade, nitrogen oxides (NO_x) [1] emissions from Diesel engines have been significantly reduced through the adoption of advanced exhaust after-treatment technologies. Among these, Selective Catalytic Reduction (SCR) systems [2] represent one of the most effective solutions for meeting increasingly stringent emission regulations.

In SCR systems, a urea–water solution (UWS) [3] is injected into the hot exhaust stream upstream of the catalytic converter. Following injection, water evaporation and urea thermochemical decomposition lead to the formation of ammonia (NH_3) [4], which reacts with NO_x over the catalyst surface, converting them into nitrogen and water. Despite the high efficiency of this technology, solid deposit formation within the exhaust line remains a critical issue. Deposits originate from incomplete evaporation or decomposition of UWS droplets and may cause flow obstruction, catalyst degradation, and performance losses, ultimately leading to complete SCR blockage within a few hours of operation under critical conditions.

Deposit formation is strongly influenced by the complex interaction between spray droplets, turbulent exhaust flow, and solid surfaces. In particular, spray–wall interaction (SWI) [5] plays a central role, as droplet impingement determines wall wetting, liquid film formation, secondary droplet generation, and local heat transfer. These mechanisms directly affect evaporation dynamics and thermal behaviour inside the exhaust duct.

Computational Fluid Dynamics (CFD) has become an essential tool for analyzing UWS injection and predicting deposit formation during the design phase of SCR systems. However, reliable predictions require accurate modeling of multiple coupled processes, including spray atomization, droplet transport, evaporation, heat transfer, thermochemical decomposition, and spray–wall interaction.

Within this framework, the present work focuses on the numerical investigation of spray–wall interaction under high-temperature exhaust conditions typical of SCR systems. A multi-region CFD approach is adopted, accounting for gas flow, conjugate heat transfer in solid walls, porous-medium representation of internal components, and Lagrangian spray dynamics. Particular attention is devoted to the analysis and comparison of advanced SWI models, with the objective of improving predictive capability in terms of liquid film formation, evaporation behaviour, and thermal coupling between droplets

and solid surfaces.

2. Methodology

The present work adopts a fully coupled multi-region CFD framework to investigate the injection of a Lagrangian spray inside a channel representative of an SCR exhaust after-treatment system. The simulations were performed combining conjugate heat transfer with an Eulerian–Lagrangian description of the dispersed phase.

2.1. Multi-Region Computational Framework

The computational domain was subdivided into four physically distinct and strongly coupled regions:

- **Fluid domain**, describing the carrier gas flow;
- **Solid domain**, representing the channel walls with conjugate heat transfer;
- **Porous domain**, modeling the wire mesh through a homogenized Darcy–Forchheimer formulation [6];
- **Lagrangian domain**, representing the injected spray droplets.

The conservation equations of mass, momentum, and energy were solved in each region with appropriate coupling conditions at the interfaces to ensure consistency of heat and mass transfer across domains.

The wire mesh was modeled using a volume-averaged porous-medium approach. The hydraulic effect of the mesh was introduced through additional source terms in the momentum equation, accounting for viscous and inertial losses without explicitly resolving the detailed geometry of individual wires. This approximation significantly reduces computational cost while preserving the macroscopic flow behavior.

2.2. Lagrangian Spray Modeling

The dispersed liquid phase was described using a Lagrangian parcel tracking approach [7]. Each parcel represents a group of droplets sharing identical thermophysical properties.

Droplet motion was obtained by integrating Newton's second law, assuming aerodynamic drag as the dominant force. The drag coefficient was evaluated through the Schiller–Naumann correlation, ensuring validity over the droplet Reynolds number range encountered in the present configuration.

Mass transfer from the liquid to the gas phase was modeled using a diffusion-controlled evaporation framework based on the classical D^2-law, with convective corrections introduced through the Ranz–Marshall correlations for Sherwood and Nusselt numbers.

The droplet energy equation was solved to account for:

- convective heat exchange with the gas phase,
- latent heat of vaporization,
- coupling between mass and heat transfer processes.

At elevated wall temperatures, the formulation switches to a boiling-controlled evaporation regime to prevent non-physical divergence of the evaporation rate near saturation conditions.

2.3. Spray Submodels

To capture realistic spray dynamics, additional submodels were activated:

- **Turbulent dispersion model**, introducing stochastic velocity fluctuations to represent droplet–turbulence interaction;
- **Secondary breakup model (Reitz–Diwakar)**, predicting fragmentation based on Weber number criteria;
- **Collision and coalescence model (O'Rourke)**, accounting for droplet–droplet interactions in dense spray regions.

These models allow consistent prediction of spray penetration, droplet size distribution evolution, and evaporation enhancement due to atomization.

2.4. Spray–Wall Interaction Modeling

A central aspect of the methodology is the comparison between two spray–wall interaction models.

Bai Model The Bai model [8] provides a predominantly kinematic description of droplet impingement. Impact regimes (deposition, rebound, splash) are determined through Weber and Laplace numbers. Secondary droplet generation is modeled through empirical correlations, while mass and energy conservation are enforced during splash events.

Kuhnke Model The Kuhnke model [9] incorporates both inertial and thermal effects. Droplet behavior is classified into deposition, rebound, splash, and thermal break-up regimes based on the Mundo number and a dimensionless wall temperature parameter. This formulation enables modeling of Leidenfrost conditions and thermally driven fragmentation.

2.5. Lagrangian Liquid Film Modeling

When deposition occurs, droplets contribute to the formation of a surface liquid film described using a thin-film approximation. The model solves surface-based conservation equations for:

- film mass,
- depth-averaged momentum,
- film energy.

Film evolution accounts for shear stress imposed by the gas phase, gravitational effects, wall heat conduction, and evaporation at the liquid–gas interface. The film formulation is fully coupled with both the gas-phase solver and the solid thermal domain, ensuring consistent prediction of wall cooling and local evaporation phenomena.

2.6. High-Temperature Regimes and Film Boiling

To describe droplet interaction at high wall temperatures, the O'Rourke film boiling evaporation model [10] was employed. The formulation accounts for transitions between convective heat transfer, nucleate boiling, transition boiling, and film boiling regimes.
Above the Leidenfrost temperature [11], the formation of a stable vapor layer reduces direct liquid–solid contact, modifying both droplet dynamics and heat transfer mechanisms. This effect is consistently integrated with the spray–wall interaction models.

3. Test Case

A simplified geometry representative of an SCR channel was adopted in order to obtain reliable numerical results while reducing computational cost.

3.1. Geometrical Configuration

Two configurations were considered: wire mesh impingement and wall impingement.

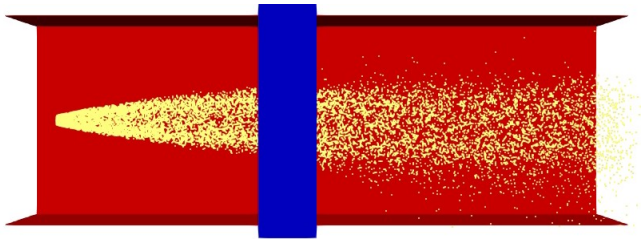

Figure 1: Wire mesh impingement configuration

Figure 1 shows the wire mesh impingement configuration. The computational domain is subdivided into three main regions:

- **Solid domain** (red), representing the structural support of the wire mesh and defining the external boundaries of the system;
- **Porous domain** (blue), modeling the wire mesh as a planar porous slab with finite thickness, perpendicular to the main flow direction and spanning the entire channel cross-section;
- **Lagrangian spray domain** (yellow), where droplets are injected and tracked within the carrier gas.

The spray originates upstream of the porous structure and develops along the axial direction, forming a conical plume centered with respect to the wire mesh to allow direct droplet impingement.

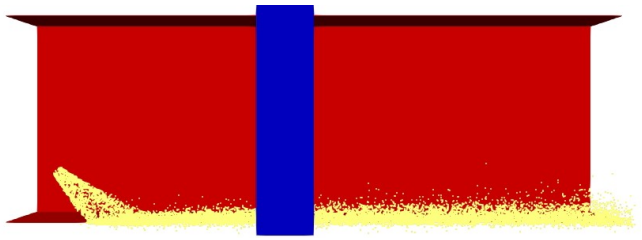

Figure 2: Wall impingement configuration

Figure 2 illustrates the wall impingement configuration. The solid and porous domains remain unchanged, while the spray is oriented toward the lower channel wall. In this case, droplets first impact the wall and are subsequently transported by the airflow toward the porous region.

3.2. Operating Conditions

The simulations were performed under operating conditions representative of realistic SCR exhaust systems.
The exhaust gas velocity was varied within 25

m/s, 50 m/s, 75 m/s and 100 m/S to reproduce different engine load conditions. This parameter strongly influences droplet trajectories, spray dispersion, impingement intensity, and residence time.
The gas temperature was varied between 200 °C 500 °C to investigate the transition between different spray-wall interaction regimes, including film formation, rebound, splash, and thermally induced breakup. Temperature directly affects evaporation kinetics and heat transfer mechanisms.
Additional simulations were conducted near the Leidenfrost threshold at 80 °C, 100 °C, 110°C and 150 °c to analyze both sub-Leidenfrost and super-Leidenfrost conditions. The Leidenfrost temperature marks the transition at which a stable vapor layer forms between the liquid and the heated surface, significantly altering heat transfer and impact dynamics.
The UWS mass flow rate was fixed at 5×10^{-6} kg/s and the injection temperature was maintained at 23°C to reproduce realistic tank conditions.
The injection duration was set to 0.013 s, corresponding to a single dosing event. The total simulation time was extended to 0.026 s to capture post-injection evaporation and thermal relaxation processes.
The injector discharge coefficient was initially set equal to 1, representing ideal hydraulic conditions. Additional simulations were performed with a reduced discharge coefficient of 0.5, while maintaining constant mass flow rate, to evaluate the influence of injector hydraulic efficiency. Reducing the discharge coefficient increases injection velocity and spray momentum, modifying droplet size distribution and aerodynamic interaction.
In the following table the main operating conditions are reported

	Velocity [m/s]	Temperature [°C]	Discharge coeff.
Case 1	50	80–100–110–150	1
Case 2	25–50–75–100	300	1
Case 3	50	200-250-300-350-400-450-500	1
Case 4	50	300–350–400	0.5

Table 1: Setup cases

4. Results and Discussion

4.1. Wall Impingement

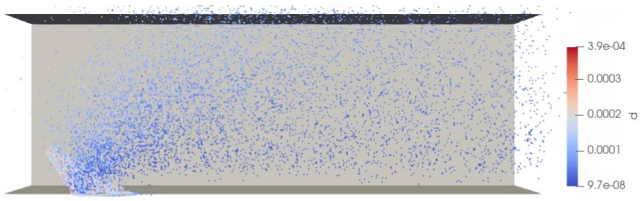

Figure 3: Lagrangian spray wall Bai

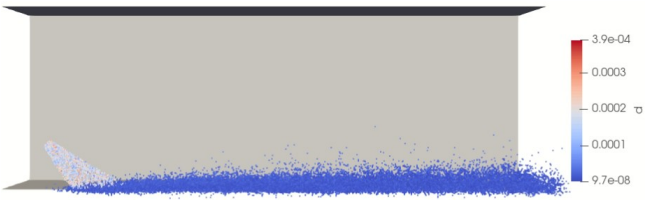

Figure 4: Lagrangian spray wall Kuhnke

Figures 3 and 4 illustrate the behaviour of the Lagrangian spray when the jet is directed towards the lower wall of the computational domain.
In Bai model droplets impacting the wall initially generate a localized accumulation region at the impact location. After the impact, droplets undergo deformation and partial energy dissipation, which leads to a rebound behaviour.
In the Kuhnke model droplets impacting the wall tend to adhere to the surface, resulting in limited rebound and reduced secondary atomization. The droplets remain attached to the wall and are subsequently transported by the shear forces generated by the surrounding airflow.

Figure 5: Wall temperature distribution Bai 80 °C

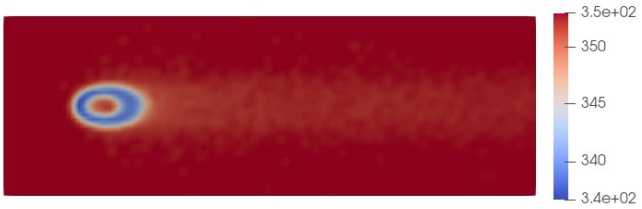

Figure 6: Wall temperature distribution Kuhnke 80 °C

By analysing the wall temperature field under operating conditions characterized by an airflow velocity of 50 m/s and an airflow temperature of 80 °C below the Leidenfrost temperature (110 °C), it is possible to observe that fluid deposition occurs at the droplet impact location for both models: droplet-wall interacttion takes place in a region in which direct contact between liquind and solid is mantained. In Bai model temperature gradient is mainly localized in the impact region, while in Kuhnke model there is a trail of liquid adhering to the wall that increases the heat exchange region.

Figure 7: Wall temperature distribution Bai 150 °C

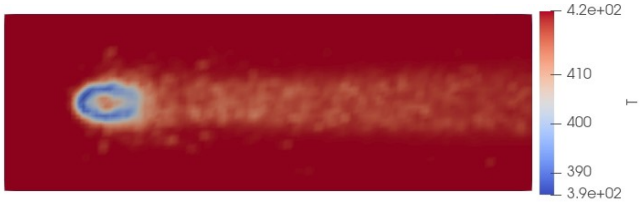

Figure 8: Wall temperature distribution Kuhnke 150 °C

Increasing the airflow temperature above the Leidenfrost temperature means that the Kuhnke model is dominated by the thermal breakup phenomenon, as we can see in figure 8. In this case the adhesion of droplets is significantly reduced and this influences the temperature gradient of the solid wall which is lower with respect to the one observed in the Bai model.

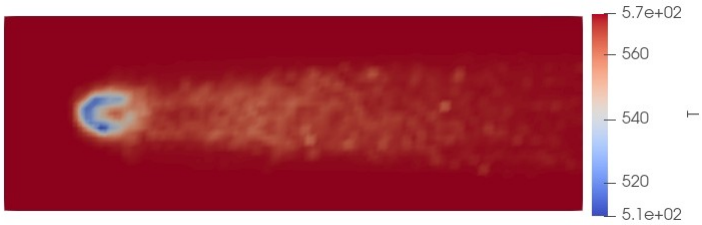

(a) 25 m/s

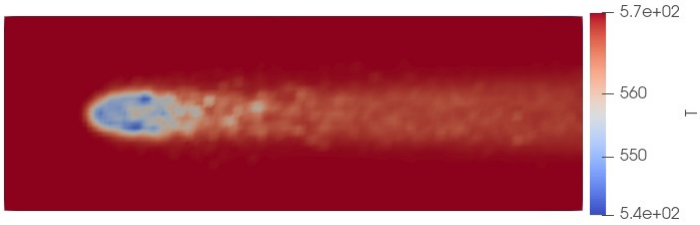

(b) 100 m/s

Figure 9: Temperature wall distribution Kuhnke

By maintaining the airflow temperature at 300 °C, it is possible to observe the effect of airflow velocity on the temperature distribution within the solid. Focusing on the Kuhnke model, we can see that, in addition to the thermal breakup phenomenon, increasing the airflow velocity enhances the aerodynamic forces acting on the droplets. This promotes greater interaction with the surrounding airflow and leads to a reduction in both the amount of liquid deposited on the impact region and the width of the liquid trail on the solid surface.

4.2. Wire Mesh Impingement

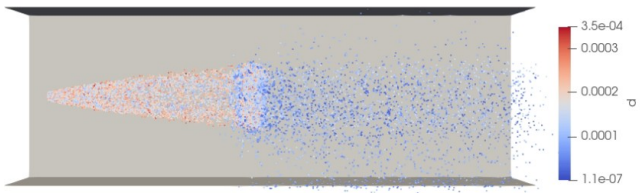

Figure 10: Lagrangian spray Bai 80 °C

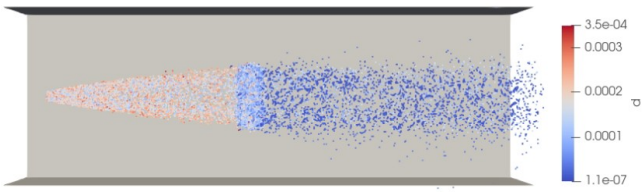

Figure 11: Lagrangian spray Kuhnke 80 °C

Fixing the air velocity to 50 m/s and the airflow temperature to 80 °C, below the Leidenfrost

temperature, both models exibit the formation of liquid film on the wire mesh. The simulation time of this case was extended to 0.05 s in order to obtain more reliable results in terms of liquid film volum and mass fraction of water evaporated.

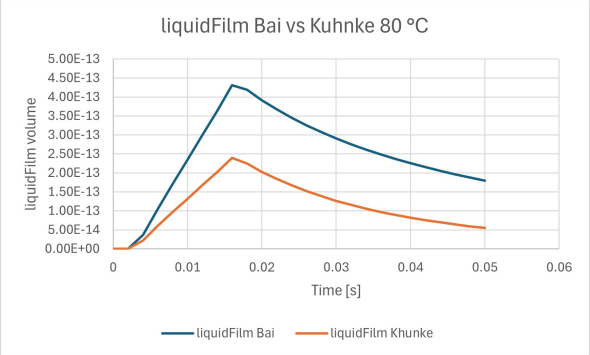

(a) liquidFilm volume 80 °C.

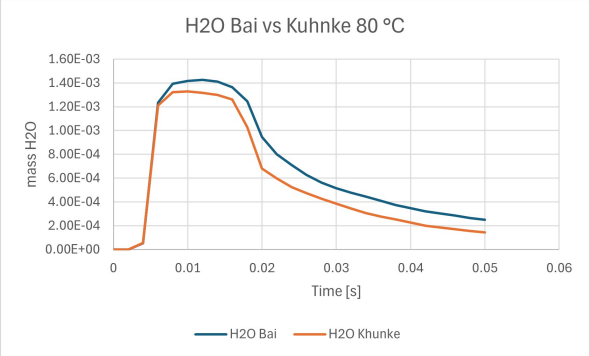

(b) Mass fraction of H_2O evaporated 80 °C K

Figure 12

Since operating temperature is under the water's boiling temperature more time is needed in order to evaporate the injected mass of H_2O

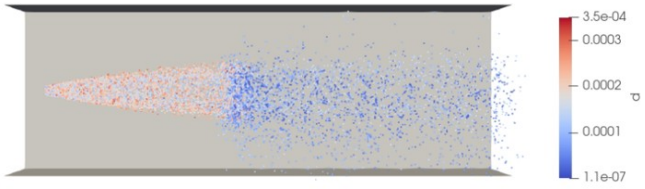

Figure 13: Lagrangian spray Bai 150 °C

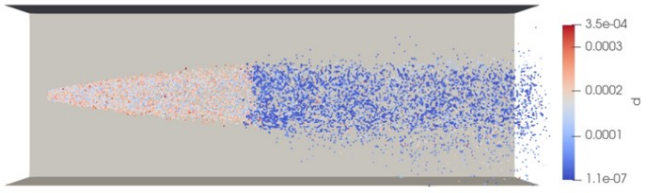

Figure 14: Lagrangian spray Kuhnke 150 °C

At 150 °C, above Leidenfrost temperature form figure 14 it's possible to notice that the Kuhnke modeòl doesn't predict any formation of liquid film on the wire mesh since the thermal breakup is the dominant phenomena, while Bai continues to predict liquid film formation on the wire mesh. The secondary parcels generated after the impact of the lagrangian spray on the wire mesh result smaller in the Kuhnke model with respect to the Bai model since in Kuhnke model the interaction is both inertial and thermal.

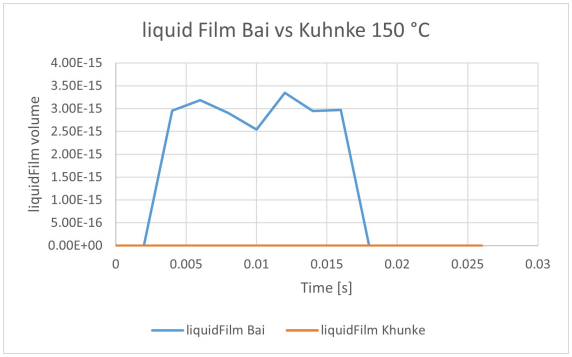

(a) liquidFilm volume 150°C.

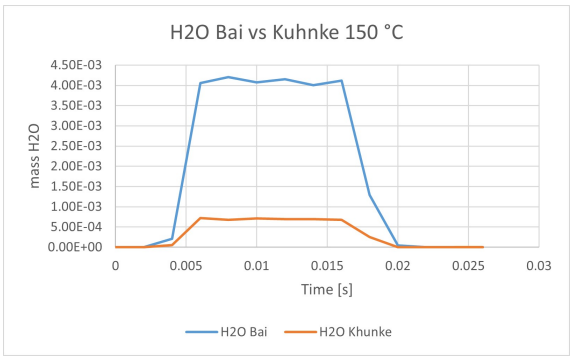

(b) Mass fraction of H_2O evaporated 150 °C.

Figure 15

figure 15a and figure 15b show that there is no water inside the system at the end of the simulation, meaning that in this case the amount of heat flux is sufficient to fully evaporate the liquid film generated.

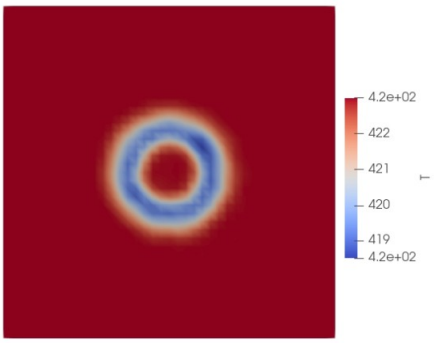

(a) Bai

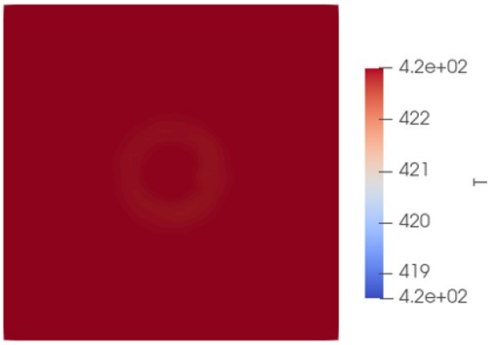

(b) Kuhnke

Figure 16: WireMesh temperature 150 °C.

Another aspect that is linked to the absence of liquid film formation on the wire mesh in Kuhnke model is the comparison of wire mesh temperature distribution shown in figure 16. In the Bai model, the presence of the liquid film results in a more pronounced temperature decrease on the wire mesh, producing a stronger and more uniformly distributed temperature gradient while, the Kuhnke model, due to the absence of liquid film formation, exhibits a lower temperature gradient along the wire mesh and a less uniform temperature distribution.
Maintaining a constant airflow velocity of 50 m/s allows the evolution of the liquid film volume to be analysed as a function of operating temperature, effectively isolating thermal effects from aerodynamic influences.

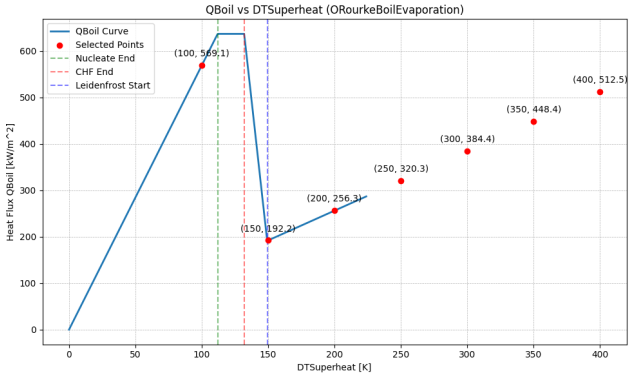

Figure 17: Operating points on the O'Rourke film boiling evaporation curve

Figure 17 reports the operating points of the investigated cases mapped onto the film boiling evaporation curve adopted in the O'Rourke model. At the lowest investigated temperatures (200 °C and 250 °C), the operating conditions correspond to regions characterized by high heat flux values, typically associated with nucleate or early transition boiling regimes.
At the higher value of temperature (400 °C, 450 °C and 500 °C) there is the formation of the vapor layer as the system is entered in the transition phase. This means that the amount of heat flux available is lower and , therefore, the liquid film volume increases. In those cases the amount of heat flux is sufficient to fully evaporate the liquid film deposited on the wire mesh
The intermediate temperatures (300 °C and 350 °C) operate in the transition region amd so the amount of heat flux is not sufficient to fully evaporate the amount of liquid film deposited on the wire mesh

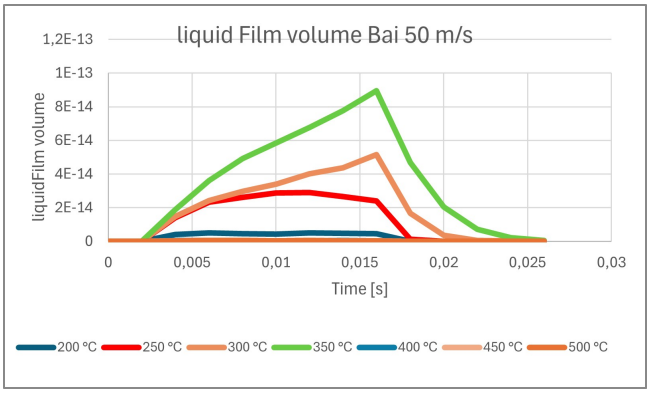

Figure 18: Liquid film Bai

This phenomenon is clearly evident in figure 18: the maximum of liquid film volume is obtained

at 350 °C because the amount of heat flux according to the O'Rourke film boiling model is the minimum available in the system.

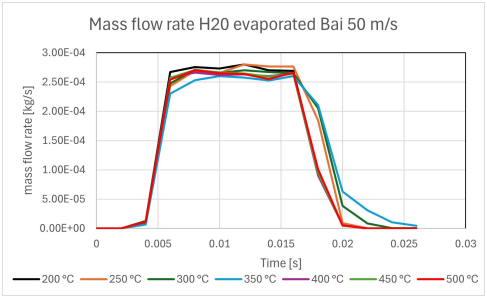

(a) Bai

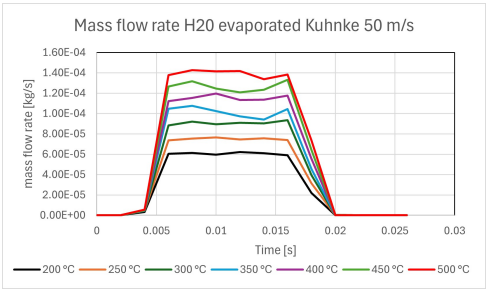

(b) Kuhnke

Figure 19: Evaporated water mass

The O'Rourke film boiling model influences also the amount of mass of water evaporated during the simulation in the Bai model. In particular at the intermediate temperature there is residual mass of water not evaporated at the end of the simulation since the amount of heat flux available is not sufficient. All the other temperature have no residual water at the end of the simulation. The evaporation velocity is higher at the higher temperature because the heat tranfer is faster in presence of higher temperature gradient.

5. Main Conclusions and Future Work

This work numerically investigated the behaviour of a Lagrangian spray injected into a channel representative of an SCR exhaust system by means of a multi-region CFD approach implemented in *OpenFOAM*. The analysis focused on the comparison between the Bai and Kuhnke spray–wall interaction models and on the influence of key operating parameters, namely air temperature, wall temperature, airflow velocity and injector discharge coefficient.

The comparison between the two wall-interaction models revealed substantial differences in droplet impact behaviour and subsequent evaporation dynamics. The Bai model, based on a predominantly kinematic formulation, tends to predict rebound-dominated behaviour and persistent liquid film formation. In contrast, the Kuhnke model incorporates both kinetic and thermal effects, allowing droplet adhesion, thermally induced breakup and stronger coupling between liquid structures and the heated surface.

Temperature was identified as the dominant parameter controlling regime transition. Below the Leidenfrost threshold, both models predict liquid film formation on the impingement surface. Above the Leidenfrost temperature, however, the predictions diverge significantly: while the Bai model continues to predict stable liquid films, the Kuhnke formulation suppresses film formation due to thermal breakup mechanisms. This leads to markedly different evaporation trends and heat transfer characteristics.

Airflow velocity strongly affects droplet residence time and overall heat exchange. Lower velocities enhance evaporation due to prolonged interaction time between droplets, walls and hot gases, whereas higher velocities reduce residence time and limit global evaporation despite increased aerodynamic transport toward the impingement surface.

The injector discharge coefficient influences both droplet size and injection velocity. A reduced coefficient promotes atomization and increases the surface-to-volume ratio, enhancing convective heat transfer. However, the associated increase in injection momentum reduces residence time. These competing mechanisms partially compensate each other, resulting in comparable global evaporation levels.

Overall, the study demonstrates that spray–wall modelling strategy, thermal conditions and aerodynamic parameters are strongly coupled and significantly affect liquid film dynamics, secondary droplet formation and evaporation efficiency in SCR-like configurations. The results underline the importance of adopting thermally consistent wall-interaction models for reliable prediction of high-temperature exhaust applications.

Possible extensions of the present work could

focus on a deeper investigation of deposit formation phenomena. In particular an accurate representation of urea thermophysical properties should be integrated together with the investigation of realistic multi-injection strategies, in order to capture the influence that each injection event exerts on the following ones. Furthermore, the development of predictive deposit-risk models is required to bridge the gap between short-duration simulations, limited to a few injection events, and real operating cycles (typical duration $>$ 10 hours), enabling a physically consistent extrapolation of long-term deposit accumulation trends based on the spray, film formation and evaporation dynamics identified in this work.

References

[1] Marek Brzezanski and Rafal Sala. The influence of adblue dosage on the process of selective catalytic reduction of nitrogen oxides. 154(3):1032–1037, 09 2013.

[2] Felix Birkhold, Ulrich Meingast, Peter Wassermann, and Olaf Deutschmann. Modeling and simulation of the injection of urea-water-solution for automotive scr denox-systems. *Applied Catalysis B: Environmental*, 70(1):119–127, 2007.

[3] Yongseok Cho, Seang-Wock Lee, W. Choi, and Y. Yoon. Urea-scr system optimization with various combinations of mixer types and decomposition pipe lengths. *International Journal of Automotive Technology*, 15:723–731, 08 2014.

[4] Sung Dae Yim, Soo Jean Kim, Joon Hyun Baik, In-Sik Nam, Young Sun Mok, Jong-Hwan Lee, Byong K. Cho, and Se H. Oh. Decomposition of urea into nh3 for the scr process. *Industrial and Engineering Chemistry Research*, 43(16):4856 – 4863, 2004. Cited by: 346.

[5] Henrik Smith, Markus Zöchbauer, and Thomas Lauer. Advanced spray impingement modelling for an improved prediction accuracy of the ammonia homogenisation in scr systems. *SAE Technical Papers*, 2015, 04 2015.

[6] Aykut Gunhan. Numerical Modeling of Porous Media Using a 3D Darcy-Forchheimer Approach. Master's thesis, Politecnico di Milano, 2023-2024.

[7] P.J. O'Rourke and A.A. Amsden. A particle numerical model for wall film dynamics in port-injected engines. *SAE Technical Papers*, 1996. Cited by: 241; All Open Access, Green Open Access.

[8] Behrad Asgari and Ehsan Amani. An improved spray-wall interaction model for eulerian-lagrangian simulation of liquid sprays. *International Journal of Multiphase Flow*, 134, 2021.

[9] Dominik Kuhnke. Spray / wall-interaction modelling by dimensionless data analysis. 2004.

[10] Mrugank P. Bhatt, Pengze Yang, and Chaouki Habchi. Numerical modeling of liquid film boiling, urea deposition and solidification in scr applications. 2024.

[11] Fabian M. Tenzer, Julian Hofmann, Ilia V. Roisman, and Cameron Tropea. Leidenfrost temperature in sprays: role of the substrate and liquid properties, 2020.

Acknowledgements

I would like to express my sincere gratitude to Professor Augusto Della Torre for his guidance, support and availability throughout the development of this work.
I also wish to thank Engineer Mattia Pelosin for his valuable technical assistance and constant support during the thesis activities.
My appreciation goes to my colleagues and friends who contributed, directly and indirectly, to making this academic journey both stimulating and rewarding.
Finally, I would like to thank my family for their continuous encouragement and unwavering support during my studies.